

# Rotational velocity fields of galaxies and projective geometry of spacetime

Jacques Rubin

► **To cite this version:**

Jacques Rubin. Rotational velocity fields of galaxies and projective geometry of spacetime. 2017.  
<hal-01637022>

**HAL Id: hal-01637022**

**<https://hal.inria.fr/hal-01637022>**

Submitted on 17 Nov 2017

**HAL** is a multi-disciplinary open access archive for the deposit and dissemination of scientific research documents, whether they are published or not. The documents may come from teaching and research institutions in France or abroad, or from public or private research centers.

L'archive ouverte pluridisciplinaire **HAL**, est destinée au dépôt et à la diffusion de documents scientifiques de niveau recherche, publiés ou non, émanant des établissements d'enseignement et de recherche français ou étrangers, des laboratoires publics ou privés.

# Rotational velocity fields of galaxies and projective geometry of spacetime

Jacques L. Rubin

Université de Nice–Sophia Antipolis  
Institut de Physique de Nice – UMR7010-UNS-CNRS  
Site Sophia Antipolis  
1361 route des lucioles, 06560 Valbonne, France  
`jacques.rubin@inphyni.cnrs.fr`

November 17, 2017

## **Abstract**

Relativistic localizing systems show that the pseudo-Riemannian geometry of spacetime is somehow encapsulated in the projective geometry of a Cartan connection space (generalized Cartan space). In this paper, we present fits of rotational velocity fields of galaxies based on a modification of the Newton's law of gravitation such that it becomes equivariant with respect to the homographic transformations induced by this projective geometry.

# 1 Introduction

In this paper, we present fits of galactic rotation curves resulting from the effect of the local projective geometry of spacetime. The existence of this geometry has been demonstrated based on only the purely metrological characteristics of systems of relativistic localization of events in spacetime [1, 2, 3]. The three-dimensional projective geometry in spacetime is well-known for velocities but the present projective geometry is a four-dimensional projective geometry relating exclusively to events. The projective theory of the relativity was mainly investigated during the first half of the 20th century but it was at that time impossible to identify the “projective” coordinates (rather called ‘homogeneous’ coordinates) to physical observables. That is certainly one of the reasons why it fell completely into oblivion [5, 6]. On the other hand, this mathematical theory was itself in full development and there was no real simple and unified presentation of it yet puzzle-like and maturing. The mathematical formalism was then presented in a very little synthetic form and difficult to access except for some mathematicians in the field.

This projective geometry that relativistic localization systems unveil is truly inherent in spacetime and somehow superimposes itself on the underlying pseudo-Riemannian geometry. Also, this projective geometry is not a consequence only of the localizing processes otherwise they would have no *connexion* with spacetime at all. More precisely, quoting A. N. Whitehead [7, Chap. IX], we can say that “... *something which is measured by a particular measure-system [the latter] may have a special relation to the phenomenon whose law is being formulated. For example, the gravitational field due to a material object at rest in a certain time-system may be expected to exhibit in its formulation particular reference to spatial and temporal quantities of that time-system.*”

## 2 The fitting procedure

In a previous article [3]-[2, see Chap. 6: Conclusion], we considered a modification of Newton’s law of gravitation so that the modified law is equivariant with respect to the homographic transformations of the time and space coordinates induced by the projective structure. More precisely, relativistic localizing systems are, in particular, sets of procedures that provide the so-called ‘emission coordinates’ of any spacetime event. Thus, these coordinates are four time type numbers for each localized event. And also, the local reference frames attached to each event are defined from four light-like vectors defining frames as elements of the light type causal class  $\{llll\}$ . Then, it can be shown that the projective geometry is manifested by homographic transformations between the emission coordinates of localized events.

Then, assuming that

- at galactic scales, the mean curvature of spacetime is vanishing,
- that due to the previous hypothesis, the passage from the emission coordinates to the Newtonian space and time coordinates is accomplished by linear transformations inherited from those between the corresponding frames of causal classes  $\{llll\}$  and  $\{ssst\}$ ,
- that the Newtonian gravitational force is also a contravariant vector for the projective geometry under consideration,

then, we can deduce that the projective geometry is also manifested at galactic scales by a subset of homographic transformations between the Newtonian space and time coordinates.

As a result, the intensity  $F_M$  of the modified Newton’s law of gravitation has the following form up to a multiplicative constant [2, 3]:

$$F_M \equiv \frac{M(r')}{r'^2}, \tag{1}$$

where

$$r' \equiv \frac{r}{(1 + a t + b r)} \quad (2)$$

results from a homography from  $(r, t)$  to  $(r', t')$  preserving the Newtonian space and time splitting and where  $t$  and  $t'$  are two “local” times (*i.e.*, times linked to the proper frame attached to each galaxy),  $M(r)$  is the mass enclosed in a sphere of radius  $r$  and  $a$  and  $b$  are constants. It should be noted that this modification nevertheless preserves the action/reaction principle contrarily to the modifications given in MOND theories [4].

Therefore, starting from the usual law for the rotational velocity field of a material body (up to a multiplicative constant):  $v(r) \equiv \sqrt{M(r)/r}$ , then we obtain after substitution of  $r$  by  $r'$ , the following general formula:

$$v_s(r, t) \equiv \sqrt{\frac{(1 + a t + b r)}{r} M\left(r/(1 + a t + b r)\right)}. \quad (3)$$

We call this velocity  $v_s$  the *scaled velocity*, hence the  $s$  index.

However, we envisage another possibility in which the substitution of  $r$  by  $r'$  in the expression of the mass  $M(r)$  is not carried out, and thus we obtain:

$$v_u(r, t) \equiv \sqrt{\frac{(1 + a t + b r)}{r} M(r)}. \quad (4)$$

We call this velocity  $v_u$  the *unscaled velocity*, hence the  $u$  index in this case.

In fact, we consider two possible justifications or hypothesis: 1) the mass distribution  $M(r)$  defines somehow a “standard” for spatial distances such as  $r$  and therefore the substitution of  $r$  by  $r'$  is effective respective to something which does not vary, *i.e.*, the mass distribution is preserved despite the substitution, and 2) the mass distribution is obtained from observational data which are already affected by a “perspective (projective) effect” which manifests itself by a first modification of distribution due to a first “observational” homography, and therefore, applying the second homography substituting  $r$  by  $r'$ , then, one returns to the unmodified, original and observational distribution  $M(r)$ .

Moreover, we can also consider these two formulas with the advantage of making it possible to discriminate what is really due, in a certain way, to a mass distribution problem which is a one-point problem or rather to a modification of the gravitational interaction which is a two-points problem.

We use observational data from the SPARC database [8, 9] with explanations of how the surface brightness densities are obtained from the ARCHANGEL software [10]. Actually, we used two sort of files directly available online on the SPARC database website, namely, the *Bulge-Disk Decompositions* files ‘XXXXXX.dens’ and the *Mass Models* files ‘XXXXXX\_rotmond.dat’ all grouped together and stored respectively in the zip files `BulgeDiskDec_LTG.zip` and `Rotmod_LTG.zip`.

Then, from the ‘XXXXXX.dens’ files, we have the surface brightness densities **SBdisk** and **SBbulge** of, respectively, the disks and the bulges of the galaxies XXXXXX with respect to the radius.

These densities are also partially given in the files ‘XXXXXX\_rotmond.dat’ but these files give less points/data to make good fits. Therefore, we use in ‘XXXXXX\_rotmond.dat’ files only the rotational velocity values **Vobs** with their error bars **errV** as functions of the radius **Rad**, *i.e.*, the variable  $r$ .

Also, we consider that the mass  $M(r)$  is given, up to a multiplicative constant, by the formula (Frederico Lelli; private communication):

$$M(r) \equiv \int_0^r \left[ \mathbf{SBdisk}(x) + \mathbf{SBbulge}(x) \right] x dx. \quad (5)$$

This formula is based on the assumption that 1) the disks of the galaxies with their possible bulges have negligible thicknesses with respect to their diameters, and 2) that the circularity defect (circular symmetry of the disks) is negligible except perhaps for extremely elliptical galaxies. Therefore, this integral is the integral of a density on a disk of radius  $r$  up to the multiplicative constant  $2\pi$  coming from the integration on the polar angle.

Then, given a galaxy XXXXXX, we apply the following sequence to produce the fit of the rotational velocity **Vobs** with respect to the radius  $r$ :

1. We make a fit of the total surface brightness density  $\mathbf{SB}(r) = \mathbf{SB}_{\text{disk}}(r) + \mathbf{SB}_{\text{bulge}}(r)$ . Typically, the functions used to make the fit are sums of functions such as  $p(r)e^{q(r)}$  or  $u(r)/w(r)$  where  $p(r)$ ,  $q(r)$ ,  $u(r)$  and  $w(r)$  are polynomials. We call this fit the *SB fit* and *SB function* the function making the fit.
2. We compute the integral (5) as a function of the primitive functions of the functions used in step 1. to make the SB fit. In other words, we compute  $M(r)$  as the primitive function of the *SB function*.
3. Then, we fit the model functions  $M(r)/r'$  or  $M(r')/r'$  to experimental data **Vobs**( $r$ ), *i.e.*, we seek for constants  $\alpha$ ,  $\beta$ ,  $\mu$ ,  $\alpha'$ ,  $\beta'$ ,  $\mu'$ ,  $\alpha''$  and  $\beta''$  which minimize the least-square errors defined from the following differences:

$$\mathbf{Vobs}(r)^2 - \frac{(\alpha'' + \beta'' r)}{r} M(r), \quad (\text{Unscaled mass case}), \quad (6a)$$

$$\mathbf{Vobs}(r)^2 - \mu' \frac{(\alpha' + \beta' r)}{r} M\left(r/(\alpha' + \beta' r)\right), \quad (\text{Scaled mass case A}), \quad (6b)$$

or

$$\mathbf{Vobs}(r)^2 - \frac{(\alpha + \beta r)}{r} M\left(\mu r/(\alpha + \beta r)\right), \quad (\text{Scaled mass case B}). \quad (6c)$$

Then, we obtain what we call the *velocity fits*. Obviously, these formulas are obtained from the formulas (3) and (4) considering the time  $t$  to be a constant included in the constants  $\alpha$ ,  $\alpha'$  and  $\alpha''$ . And either of the two ‘scaled mass cases **A** and **B**’ formulas (6b) and (6c) are used depending on the convergence difficulties encountered in the fit with respect to the constants  $\mu$  and  $\mu'$ . The latter are not related to the homographies and the qualitative shapes of the curves but there are necessary for the scaling adjustment only of the theoretical curves with the experimental data. Therefore, only the ratios  $\alpha/\beta$ ,  $\alpha'/\beta'$  and  $\alpha''/\beta''$  could have a physical content provided, however, that the time  $t$  incorporated in the constants  $\alpha$  can be fixed.

Below we represent the different ‘velocity fits.’ The fits with respect to formulas (6b) or (6c) are represented by red curves while the fits with respect to formula (6a) are represented by green curves.

As an example of fit result, the fit of galaxy NGC6503 (Fig. 1) gives the following result for **SB**( $r$ ) and for the values of coefficients  $\alpha$ ,  $\beta$ , etc.:

$$\mathbf{SB}(r) = \frac{(0.7 + 14.9x + 358.63x^2 - 94.95x^3 + 9.3x^4)}{(1 - 19.715x + 1361.3x^2 + 297.4x^3 - 698.3x^4 + 328.05x^5 + 37.5x^6)},$$

$$\begin{aligned} \alpha'' &= 2.41362, & \beta'' &= 1.70300, \\ \alpha &= 6.36509, & \beta &= 2.14073, & \mu &= 6.48990, \end{aligned} \quad (\text{Scaled mass case A}).$$

Also, among the 175 galaxies in the SPARC database, we have prioritized the least elliptical galaxies possible. The column 2 in table “SPARC\_Lelli2016c.mrt” (see link called ‘Table1.mrt’),

given on the SPARC database website, indicates for each galaxy its type in the Hubble classification. We therefore mainly chose galaxies of types S0, SA, SAB or SB (unfortunately, there are no type E galaxies in the SPARC database) or those with significant experimental points for **Vobs**.

### 3 Conclusion

Finally, regardless of any interpretation in terms of projective geometry and equivariance of the modified Newton's law (1) and if many other fits are possible in addition to those presented in this article, it would then be necessary to understand the origin of such a simple modification of Newton's law which ultimately depends only on no more than two significant parameters with respect to the curves that can be deduced in full generality.

In addition, it would also be interesting to know the optimal ratio between the part due to the disk and that due to the bulge, as is the case in formula (5), in order to make the best fits if these are still possible for other galaxies.

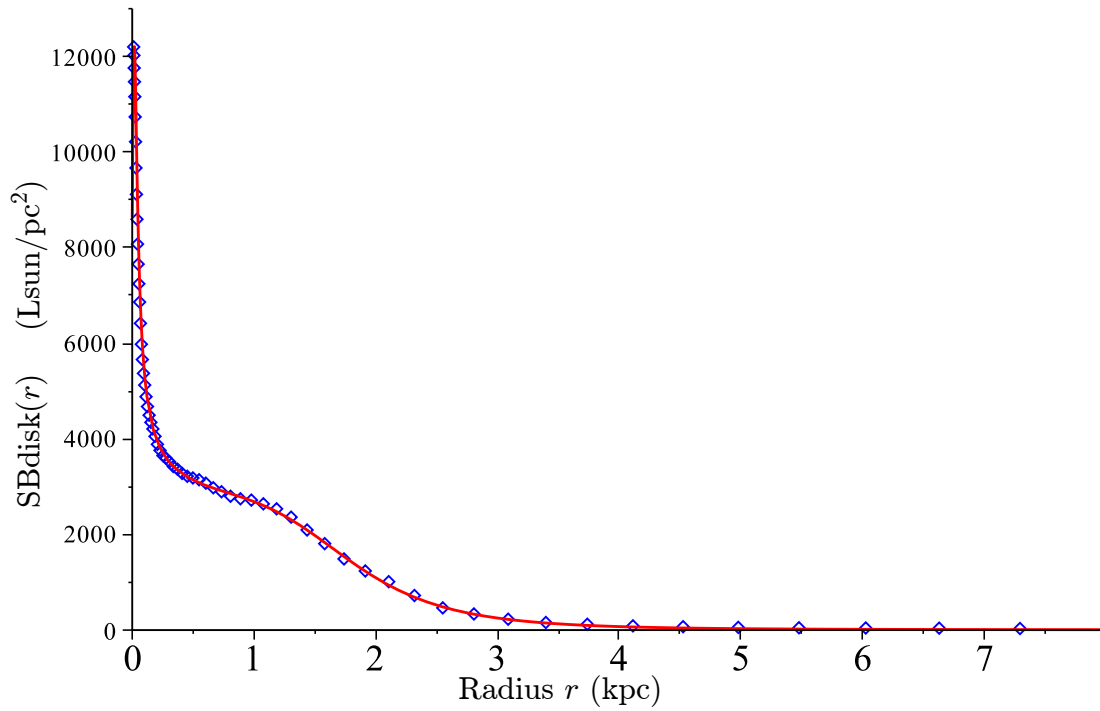
Moreover, it would be interesting to see if there is a relationship between the dependence in time  $t$  of the modified Newton's law (1) and models of accelerated expansion of the universe or galaxies clusters dynamics.

### Acknowledgement

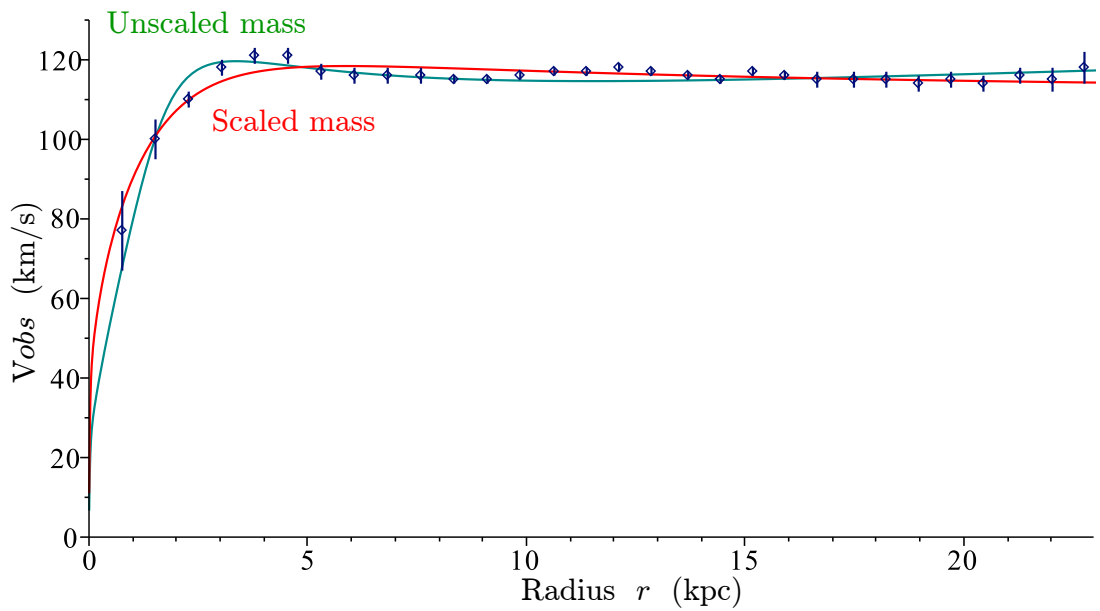
The author would like to thank Frederico Lelli (European Southern Observatory) for his suggestions of formulas for the determination of total surface brightness density (**SB<sub>tot</sub>**) and his advices. The author would also like to thank Ralf Hofmann (University of Heidelberg) and Thierry Grandou (Université de Nice - Sophia Antipolis) for their criticisms and discussions on this subject at the ICNAAM conference where a non-detailed presentation of this work was presented at the Session-Workshop: 'Nonperturbative Quantum Field Theory III,' organized by Ralf Hofmann.

## References

- [1] J. L. Rubin. Relativistic Pentametric Coordinates from Relativistic Localizing Systems and the Projective Geometry of the Spacetime Manifold. *Electronic Journal of Theoretical Physics* 12, vol. 32 (2015) 83–112.
- [2] J. L. Rubin. Relativistic localizing processes bespeak an inevitable projective geometry of spacetime. In: *Nonperturbative Approaches in Field Theory* (Eds: Ralf Hofmann and Thierry Grandou) of *Advances in High Energy Physics*, Volume 2017 (2017), Article ID 9672417.
- [3] J. L. Rubin. Consequences in fields theory and astrophysics of a projective theory of relativity emerging from relativistic localizing systems. To appear in: *Proceedings of the International Conference on Numerical Analysis and Applied Mathematics 2017 (ICNAAM-2017)*, AIP Conference Proceedings, (Session-Workshop: Nonperturbative Quantum Field Theory III. Organizer: Ralf Hofmann), 2017.
- [4] B. Famaey and S. S. McGaugh. Modified Newtonian Dynamics (MOND): Observational Phenomenology and Relativistic Extensions. *Living Review in Relativity*, **15** (2012) 10.
- [5] O. Veblen and B. Hoffmann. Projective Relativity. *Physical Review*, **36**(5) 810–822 (1930).
- [6] J. A. Schouten. La théorie projective de la relativité. *Annales de l'Institut Henry Poincaré*, tome 5, n° 1, p. 51–88 (1935).
- [7] A. N. Whitehead. *The Concept of Nature*. Tarner lectures. Cambridge University Press, Cambridge, UK, 1920.
- [8] SPARC database is maintained by Federico Lelli. Last update: 17 July 2017. <http://astroweb.cwru.edu/SPARC/>
- [9] F. Lelli, S. S. McGaugh and J. M. Schombert. SPARC: Mass Models for 175 Disk Galaxies with Spitzer Photometry and Accurate Rotation Curves. *The Astronomical Journal*, **152**(6): 157(14pp) (2016).
- [10] J. Schombert. ARCHANGEL: Galaxy Photometry System. Astrophysics Source Code Library, ASCL record: 1107.011, July 2011. <http://abyss.uoregon.edu/~js/archangel/>



(a) Surface brightness density  $\mathbf{SB}(r) = \mathbf{SB}_{\text{disk}}(r) + \mathbf{SB}_{\text{bulge}}(r)$ . ( $\mathbf{SB}_{\text{bulge}}(r) = 0$ ).



(b) Rotational velocity curve.

Figure 1: NGC6503 - Type SAcd.



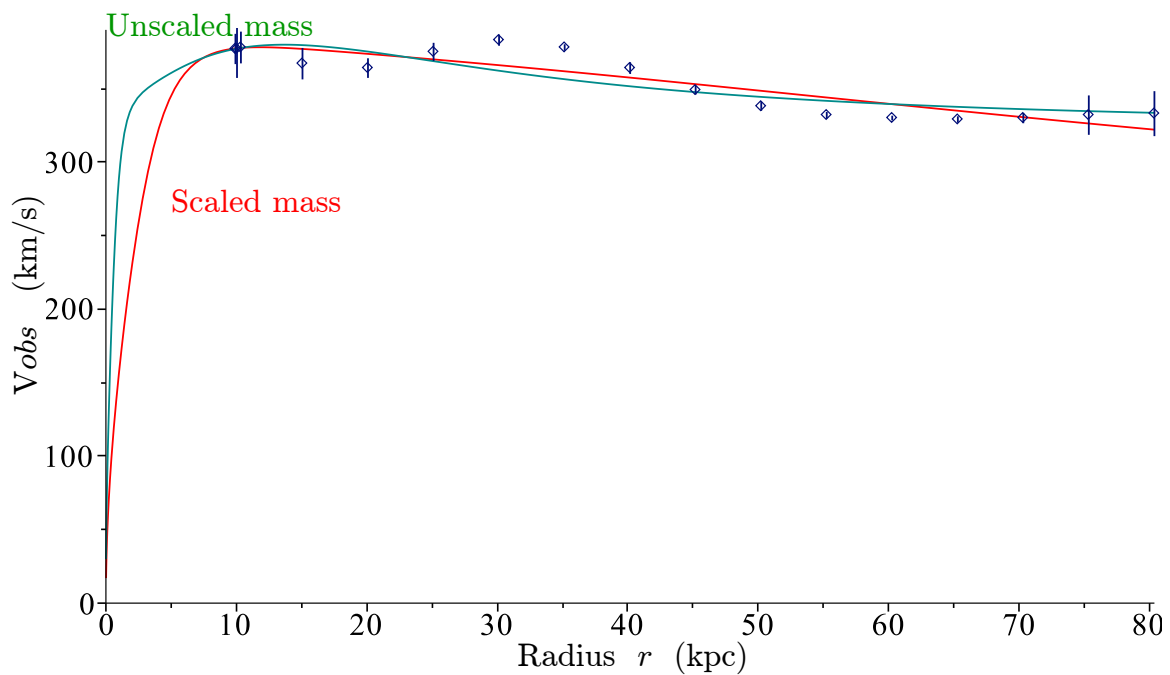


Figure 2: UGC02487 - Type S0A. ( $SBbulge(r) \neq 0$ ).

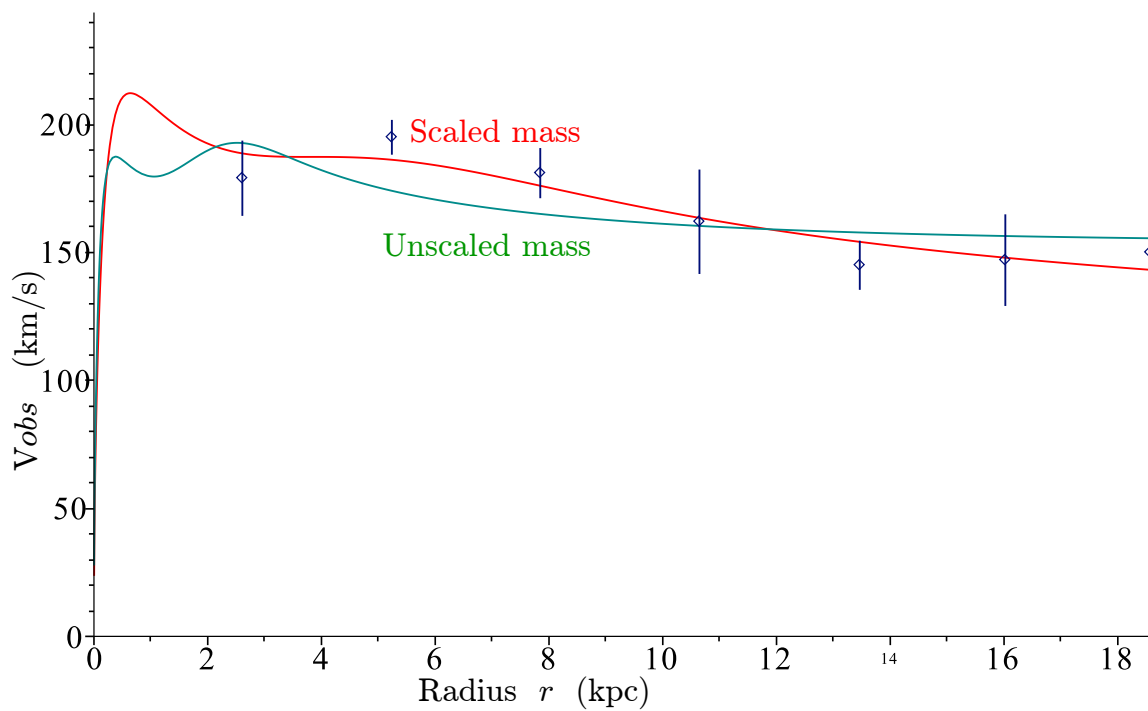


Figure 3: NGC4138 - Type S0A. ( $SBbulge(r) \neq 0$ ).

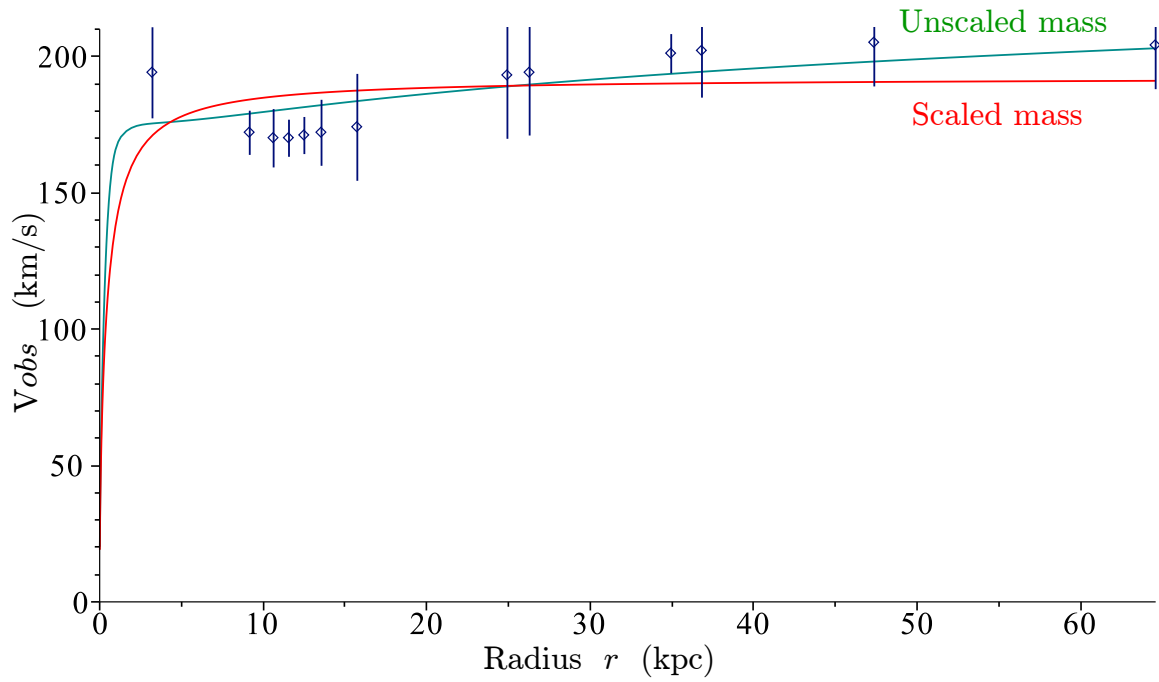


Figure 4: UGC06614 - Type SAa. ( $SBbulge(r) \neq 0$ ).

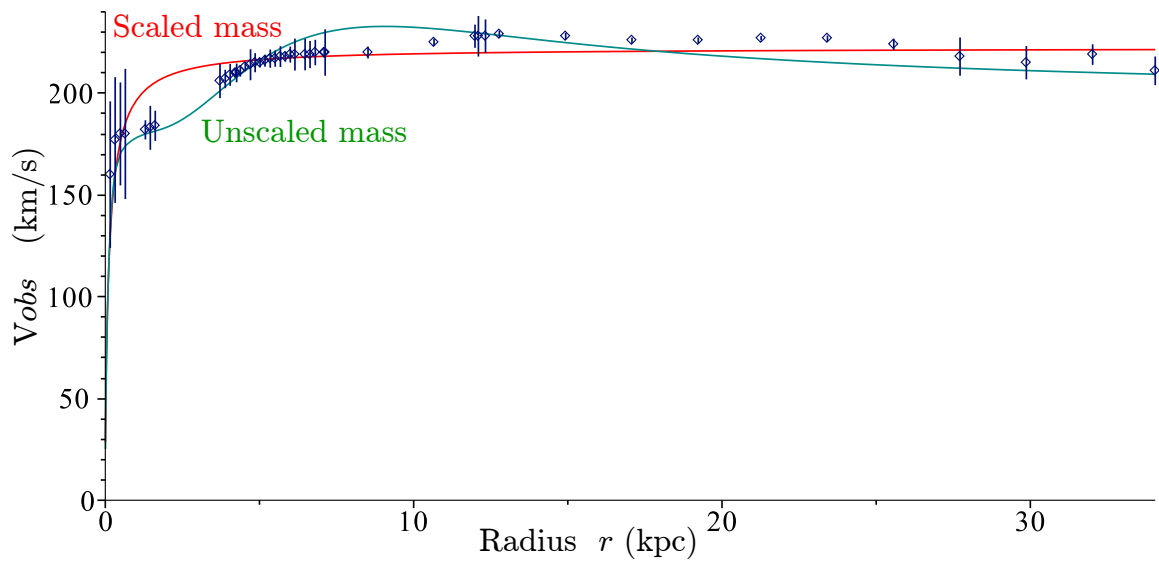


Figure 5: UGC06786 - Type SAa. ( $SBbulge(r) \neq 0$ ).

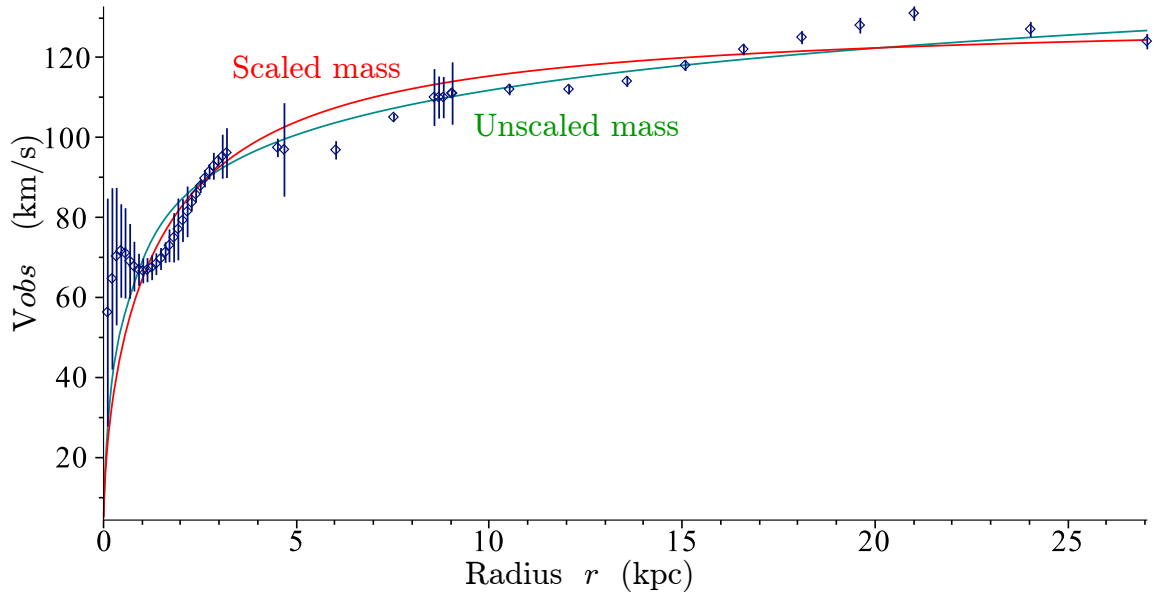


Figure 6: UGC03580 - Type SAa. ( $SBbulge(r) \neq 0$ ).

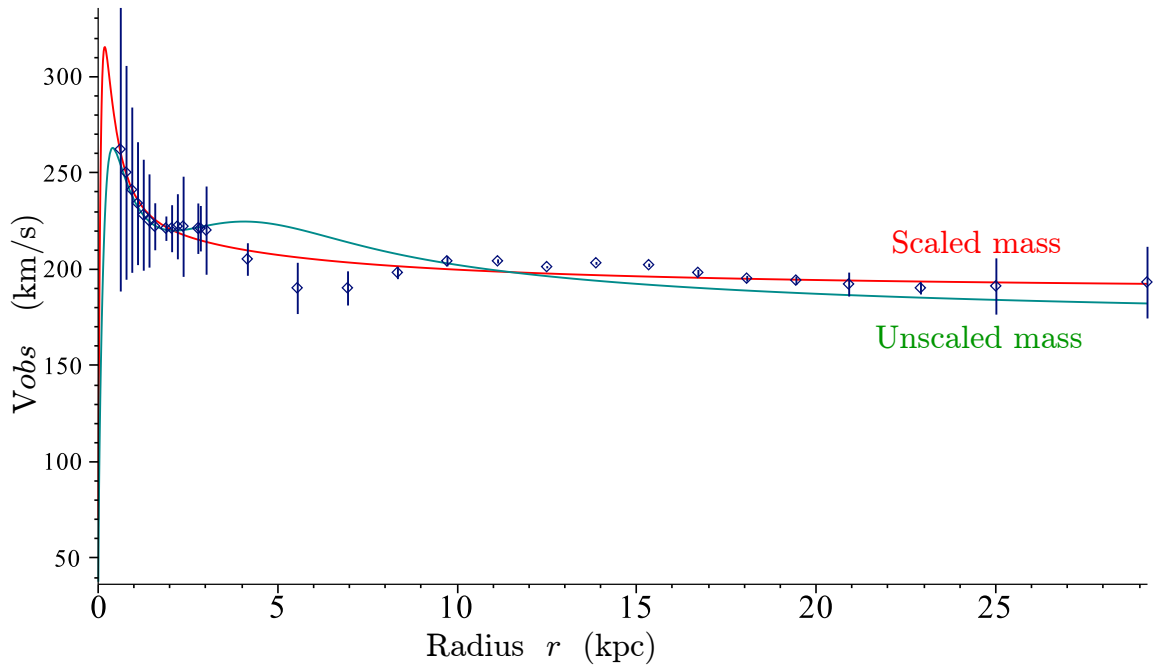


Figure 7: UGC03546 - Type SBa. ( $SBbulge(r) \neq 0$ ).

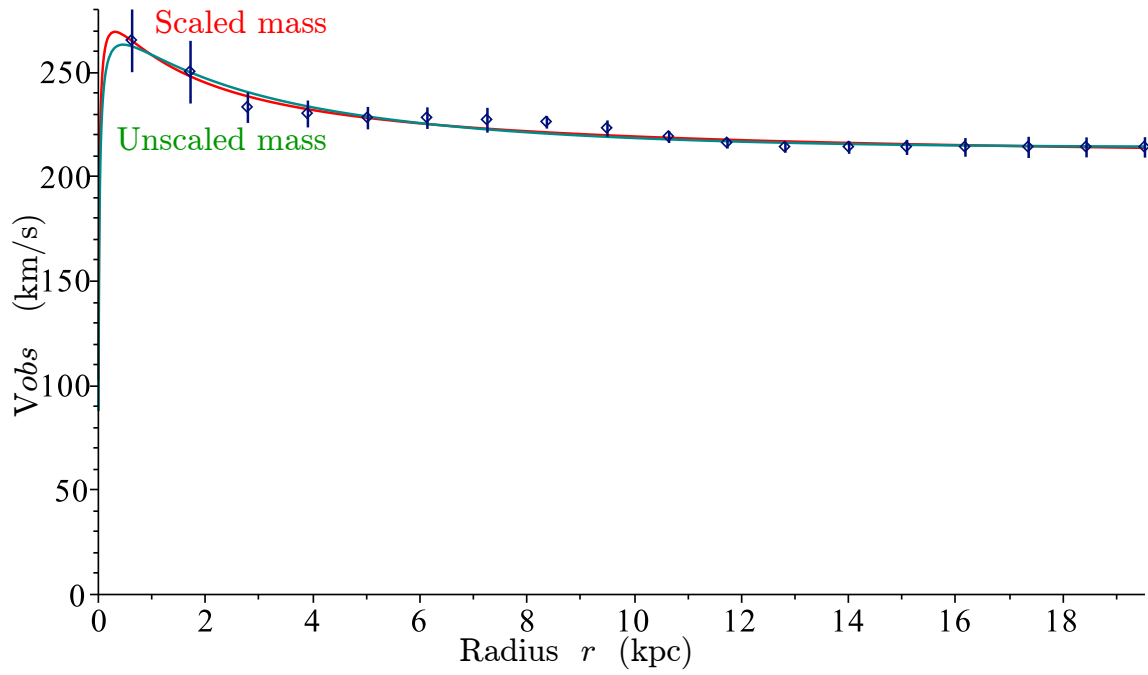


Figure 8: NGC7814 - Type SAab. ( $SBbulge(r) \neq 0$ ).

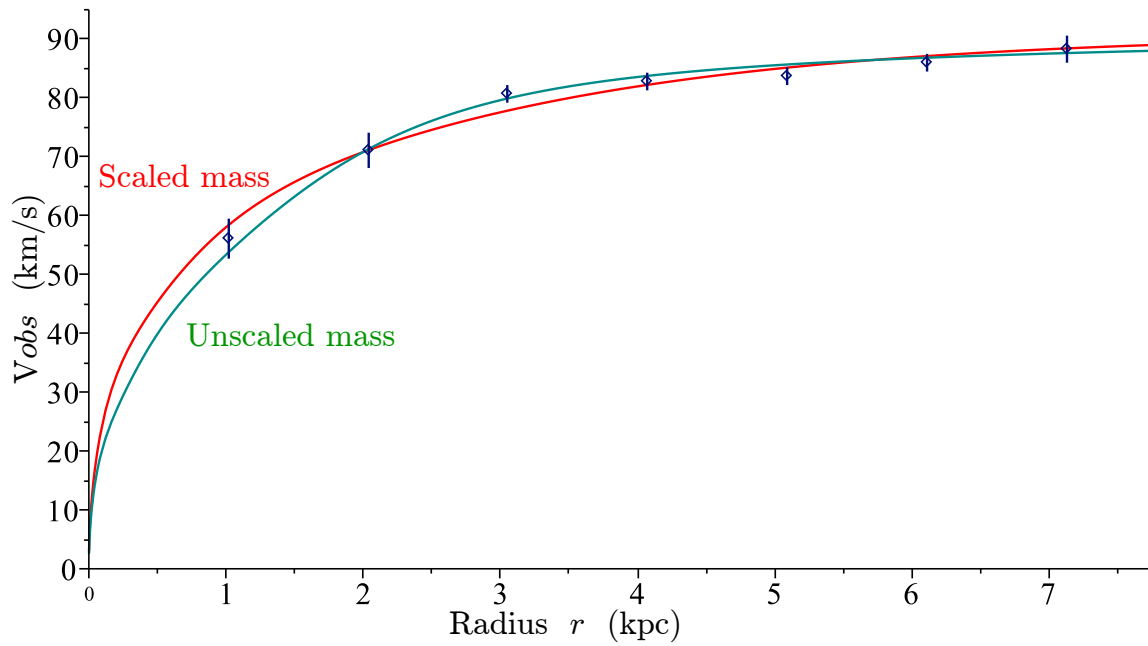


Figure 9: UGC02259 - Type Sdm. ( $SBbulge(r) = 0$ ).

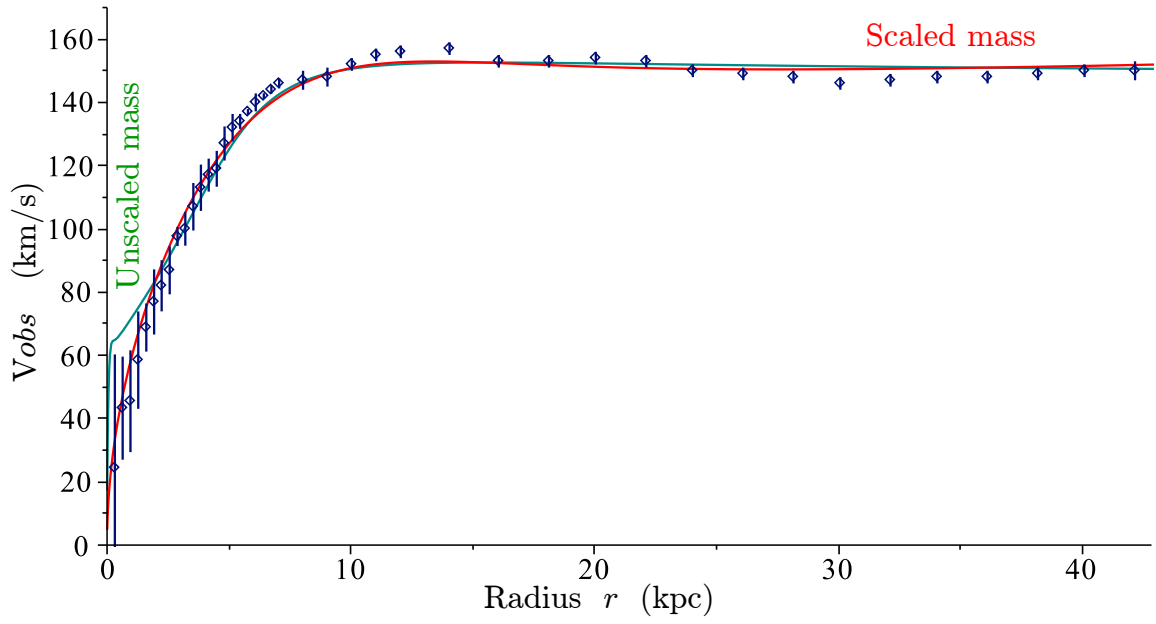


Figure 10: NGC3198 - Type SAc. (SBbulge( $r$ )= 0).

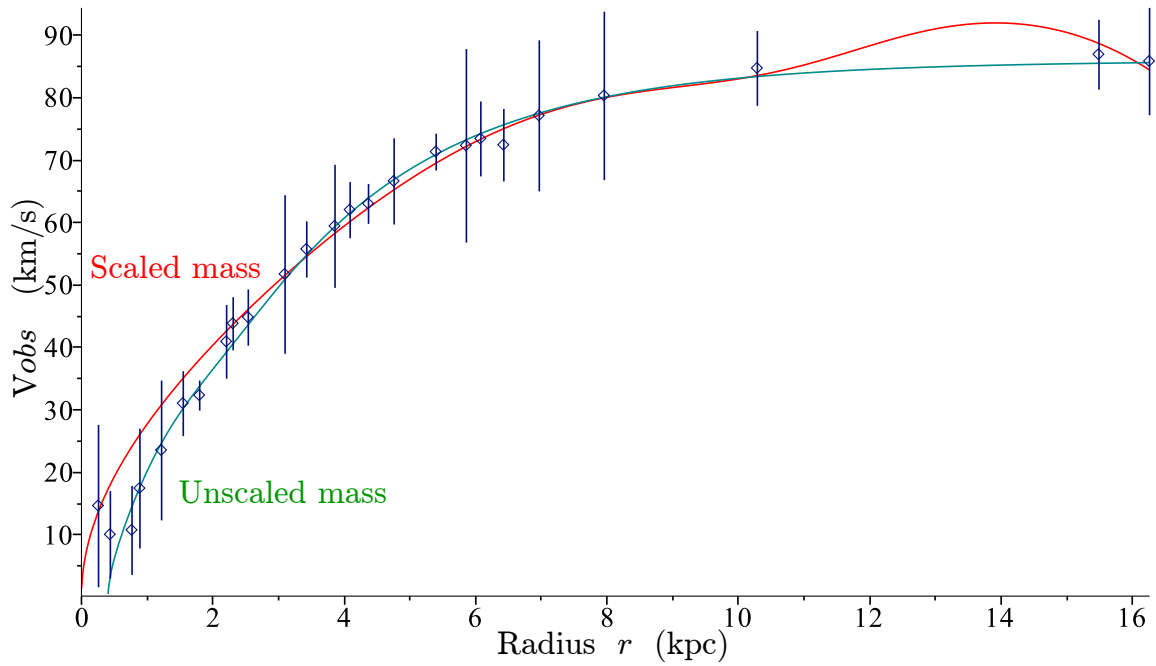


Figure 11: LSBC F583-01 - Type Sm. (SBbulge( $r$ )= 0).